Pole force and inertial measurements to analyse cross-country skiing performance in field conditions

Journal Title
XX(X):2–26

DOI: 10.1177/ToBeAssigned
www.sagepub.com/
SAGE

Antti Nikkola[1], Olli Särkkä[1], Saku Suuriniemi[1], and Lauri Kettunen[2]

Abstract

This study investigates the fusion of pole force measurement, inertial speed measurement, and video analysis to determine cross-country skiing performance in field conditions. As a proof of concept, a preliminary study was performed with different grip designs and double poling technique. The test showed that with exploiting inertial measurements, the average speed could be determined for any number of full cycles or separately for each cycle, which may be difficult with other methods in field conditions. The exploited measurements were appropriate for determining the key characteristics of the double poling cycle, which along with the estimated speed data, can be used for comparing skiing economy, determining maximum performance, and finding differences in ski equipment.

Keywords

Double poling, inertial measurements, cycle frequency, pole angle, biomechanics, cross-country skiing

Introduction

Many studies in cross-country skiing aim to gain a better understanding of the factors affecting performance. Equipment manufacturers, coaches, and the athletes themselves seek for approaches that make it possible to compare different equipment and skiing techniques. Preferably, such measurements are easy to obtain in field conditions.

In general, two important factors determine skiing performance: economy and maximum performance. In long distance races, the most important aspect is the economy of motion. Economy corresponds to the amount of work done per unit distance. Economy can be estimated, for example, by measuring oxygen consumption.[1] Maximum performance is related to the portion of maximum mechanical power that can be exploited to forward motion. Maximum performance can be measured as the maximum achievable speed, which is especially important during sprints and the finish of mass start events.

Several methods have been proposed to study skiing performance, both in laboratory and field conditions. Skiing studies often include measured force and various physiological characteristics, such as muscle activation, oxygen consumption, heart rate and blood lactate concentration.[2–6] A popular method[7–11] of studying skiing performance has entailed laboratory measurements on a treadmill using roller skis.

In this paper, the main interest was double poling (DP) performance, which can be measured with an upper-body ergometer[12;13]. Heil et al.[12] employed a specialized testing ergometer to compare different grip designs in laboratory conditions. The ergometer was used to measure the maximum DP upper body power production. The method described in the study gives direct information about the power

[1]Department of Electrical Engineering, Tampere University of Technology, P.O. Box 692, FI-33101 Tampere, Finland [2]Faculty of Information Technology, University of Jyvaskyla, P.O. Box 35, FI-40014 Jyvaskyla, Finland

Corresponding author:
Antti Nikkola, Department of Electrical Engineering, Tampere University of Technology, Tampere, Finland.
Email: antti.nikkola@gmail.com

Prepared using sagej.cls

output, which is a good indicator of performance. However, tests with an ergometer require specialised equipment that are not feasible in field conditions.

In this study, the authors focused on measuring the DP technique and instantaneous speed of the skier in the field conditions by simultaneously exploiting inertial measurements (accelerometers and gyroscopes) and pole force measurements. The accelerometers and gyroscopes were attached to a rigid roller ski, and employed inertial measurements for a different purpose and with a different approach than in previous studies. Fasel et al.[14]exploited inertial measurements to estimate the instantaneous speed of the ski and cycle characteristics of diagonal stride in classical cross-country skiing on a treadmill. Breitschädel et al.[15] studied ski glide tests exploiting inertial measurements, and Myklebust, Losnegard, et. al.[16–19] analysed cross-country skiing kinematics and techniques. Physiological characteristics can also be measured in field conditions as shown by Mahood et al.[20], but these types of measurements were not considered in this study.

Speed measurement are crucial in field tests, since, for example, the comparison of impulses or forces is futile without information about the speed that is associated with the effort. The main advantage of inertial speed measurement over light gates or video analysis is the instantaneous speed obtained with a high sampling frequency. Skiing is a cyclic motion and the skier's velocity varies substantially during one poling cycle. Thus, in order to gain representative estimates of the average speed, the speed should be calculated over several full cycles. Using light gates or video analysis is difficult because the distance over which the speed is calculated has to be selected in advance. With inertial measurements, the measurement range can be selected afterward from the gathered speed data, thus allowing additional flexibility in determining the speed measurement. Average speed can, for example, be calculated separately for each cycle.

The aim of this study was to demonstrate that inertial measurements, combined with force measurements, are a feasible approach in estimating speed and comparing maximum performance in cross-country skiing in field conditions. Another goal was to develop simple field testing methods for coaches and equipment manufacturers. Special areas of interest included the skiing speed, pole

angle to estimate the horizontal pole force during the poling phase, and differences in ski equipment. For a demonstration, a field test with two different handgrip designs was conducted. In addition, the concept to compare glide properties of the skis in DP was introduced in this study. To the best knowledge of the authors, a method capable of cycle-by-cycle speed measurement, combined with the pole force measurements, has not been previously studied in skiing. This is a topical issue, as all modern smartphones include inertial sensors and the technology needed for the measurements, data processing, and computations presented in this study.

Methods

Measurements

In this section, pole force measurements, inertial measurements, and video recordings are discussed in detail.

Pole force measurements A uniaxial load cell was used to measure pole forces. The principle is well described by Bortolan et al.[21] A small button load cell manufactured by Strain Measurement Devices[22] weighing 13 g was installed in an aluminium case weighing 48 g. The load cell used four strain gauges in full bridge configuration. This device was mounted on carbon racing poles directly below the grip. The grip was attached to the top of the aluminium case with a screw in the side of the grip and could be easily changed. Values were recorded with a portable data logger with 1 kHz per channel. The measurement device is presented in Fig. 1a.

A specific calibration stand (Fig. 1c) was used to calibrate the load cells before each measurement. The pole was placed vertically into the stand under an aluminium platform and different standard weights were placed on the platform. Calibration measurements were made without any weight and with the weight of the platform (2.236 kg) and with three standard weights (5, 10, 15 kg) in addition to the weight of the platform.

(a) A separate load cell can be seen below the poles. The data logger is above right. Above left is the standard grip and below left is the hinged grip. Both were used in the field tests.

(b) The roller ski with the IMU in front of the binding.

(c) The calibration stand (on the left) and the cube (on the right) were exploited to calibrate the load cells and inertial sensors, respectively.

Figure 1. The force measurement device (a), IMU (b), and calibration equipment (c).

In calibration of the load cells, the scale factor c and bias b were estimated from the sensor error model $y = cx + b$, where y is the measured force and x is the force due to the standard weight. The calibration measurements were exploited to form an overdetermined system of linear equations and the bias and scale factor were estimated by means of linear least squares. The standard deviations of the residual describes how well the sensor error model fits to the calibration measurements. For the load cell in the right and left pole, the standard deviation of the residuals were 1.15 N and 0.24 N, respectively.

Inertial measurements A custom made inertial measurement unit (IMU) was used to collect inertial data needed to compute the skier's instantaneous speed. The IMU unit weighed 225 g with the battery

and the aluminium cover. A similar IMU was also exploited to analyse javelin throwing mechanics.[23] In general, inertial navigation exploits acceleration and angular velocity measurements to find the position, velocity, attitude, and angular velocity of an object.[24] The IMU contained an accelerometer[25] and an angular velocity sensor[26] triad, measuring acceleration and angular velocity at 1 kHz sampling rate. The measurement data was stored to the IMU's memory.

The IMU was attached to the right roller ski also shown in Fig. 1b. It would have been impossible to attach the IMU to the centre of mass because the skier changes his position considerably while skiing, and thus, the position of his centre of mass also changes and can be outside the skier's body.

Since the test was made on a horizontal plane along a straight line and the attitude of the ski did not change significantly on DP, in this case the velocity of the ski was computed from the acceleration data in the direction of motion (parallel to the longitudinal axis of the ski).

In order to improve the measurement accuracy, the sensors were calibrated before each measurement. The technical details of the exploited calibration method are presented by Särkkä et al.[27] and are summarized below.

The purpose of calibration was to find as many deterministic sensor errors as possible. For accelerometers, the sensor error model included the biases, scale factors, misalignments, and cross-coupling errors. Stochastic errors were assumed to be normally distributed with zero expectation. The variance of the noise of the accelerometers was in the order of 10^{-4} $(\mathrm{m/s^2})^2$.

The accelerometer triad was calibrated based on multi-position calibration, where sensors were kept in a number of different positions with respect to a reference signal.[24;28] The calibration device (a cube) is presented in Fig. 1c. In this case, the reference signal was the local gravity. The IMU was installed inside the cube, which was rotated in 24 different positions. In each position, the local gravity was measured for approximately 5 seconds (5000 samples per sensor at 1 kHz). The averages of the measurements at each position constituted the calibration measurements.

The exploited sensor error model, together with the gathered calibration measurements and reference signals, constitute an overdetermined non-linear equation, which was solved with the method of least

squares in the order of a few seconds. The deterministic sensor errors were estimated and further used to adjust the raw acceleration measurements.

The position and speed were estimated from the adjusted acceleration measurements and additional position observations. The technical details can be found in the study by Nieminen[29] and are summarized below.

The speed v and position p satisfies the differential equation shown in Eq.(1)

$$\begin{cases} \dot{v} = a \\ \dot{p} = v \end{cases}, \tag{1}$$

where a is the acceleration. To estimate the speed and position from the finite data set of acceleration measurements, Eq. (1) needed be solved numerically. Equation (1) was approximated with the *trapezoidal rule*[30], which is symmetric for forward and backward processes. This property is exploited here, as the speed and position are estimated over the whole interval at once. The trapezoidal rule leads to the following residual equation shown in Eq. (2)

$$\mathbf{A}\boldsymbol{x} - \boldsymbol{b} = \boldsymbol{r}_1, \tag{2}$$

where matrix $\mathbf{A}$ is

$$\mathbf{A} = \begin{bmatrix} -1 & 0 & 1 & & & & \\ -\frac{h}{2} & -1 & -\frac{h}{2} & 1 & & & \\ & 0 & -1 & 0 & 1 & & \\ & & \ddots & \ddots & \ddots & \ddots & \\ & & & -\frac{h}{2} & -1 & -\frac{h}{2} & 1 \end{bmatrix}$$

and $h = t_{i+1} - t_i$ is the time step between successive measurements. The entries of vector $\boldsymbol{x} = [v_1\ p_1\ v_2\ p_2\ \ldots\ v_N\ p_N]^T$ are the speed v_i and position p_i to be solved at the N time instances at which

acceleration was measured. The entries of $\boldsymbol{b} = \left[\frac{1}{2}(a_1 + a_2)\ 0\ \frac{1}{2}(a_2 + a_3)\ 0 \ldots\ \frac{1}{2}(a_{N-1} + a_N)\ 0\right]^T$ are the measured accelerations a_i, $i = 1, \ldots, N$, and $\boldsymbol{r}_1$ is the residual.

The residual Eq. (2) is underdetermined with N measurements and $N - 2$ equations. For this reason, additional speed $\boldsymbol{v}^\star$ and position $\boldsymbol{p}^\star$ observations such as the initial position, zero initial speed and end position were exploited to come up with supplementary residual equations as shown in Eq. (3)

$$\begin{bmatrix} \mathbf{B} \\ \mathbf{C} \end{bmatrix} \boldsymbol{x} - \begin{bmatrix} \boldsymbol{v}^\star \\ \boldsymbol{p}^\star \end{bmatrix} = \boldsymbol{r}_2\,, \tag{3}$$

where binary matrices $\mathbf{B}$ and $\mathbf{C}$ associate the velocities and positions in $\boldsymbol{x}$, with $\boldsymbol{v}^\star$ and $\boldsymbol{p}^\star$, respectively. Compiling the residual Eqs. (2) and (3) together results in Eq. (4)

$$\mathbf{D}\boldsymbol{x} - \boldsymbol{c} = \boldsymbol{r}\,, \tag{4}$$

where $\mathbf{D} = \left[\mathbf{A}^T\ \mathbf{B}^T\ \mathbf{C}^T\right]^T$, $\boldsymbol{c} = \left[\boldsymbol{b}^T\ \boldsymbol{v}^{\star T}\ \boldsymbol{p}^{\star T}\right]^T$ and $\boldsymbol{r} = \left[\boldsymbol{r}_1^T\ \boldsymbol{r}_2^T\right]^T$.

To estimate $\boldsymbol{x}$, a linear least squares problem as shown in Eq. (5)

$$\hat{\boldsymbol{x}} = \underset{\boldsymbol{x}}{\operatorname{argmin}} \left\{\boldsymbol{r}^T\boldsymbol{r}\right\}, \tag{5}$$

is solved[31] yielding Eq. (6)

$$\hat{\boldsymbol{x}} = \left(\mathbf{D}^T\mathbf{D}\right)^{-1}\mathbf{D}^T\boldsymbol{c}. \tag{6}$$

The linear least squares method assumes the measurement errors are uncorrelated and homoscedastic with the same variance.

In the test examples, the initial position was set to zero and additional time stampings for position observations at 40 m, 60 m, and 80 m from the starting point were employed. These were obtained from video recordings. The additional position time stampings, together with the zero initial speed, make it

possible to solve $\boldsymbol{x}$ from a boundary value problem. In the test cases, $\boldsymbol{x}$ was solved in the domain from 0 to 80 m with the zero initial speed and the additional position time stamps given as additional constraints for the solution. In principle, the approach makes it possible to exploit any speed, at any instance of time, but in this case only the initial speed was available in the domain from 0 to 80 m.

Positions and speeds (i.e., $\boldsymbol{x}$) were solved as a post processing task after all the data was gathered. The solution takes a few seconds of CPU time from most computers.

The position observations with time stamps guarantee the average speed over the whole region between the boundary conditions is correct up to the measurement accuracy. The proposed approach is about solving the moments, which are time stamps of when the measurement unit was at each point within the region and what was the momentary speed at that moment. This is an optimal approach in the sense that while the average speed is correct, the momentary speeds become specified by minimizing the error in kinetic energy. In other words, the cumulative error in kinetic energy over the whole domain becomes minimized.

In case of the test run results, the initial speed and the average speeds between 0-40 m, 40-60 m, and 60-80 m were correct up to the measurement error. The momentary speeds in the subdomains 0-40 m, 40-60 m, and 60-80 m were solved from the accelerations, such that the error in kinetic energy was minimized in each subdomain.

As in all position and velocity measurements, the absolute error is difficult to estimate. The absolute error depends on the accuracy of the time stamped positions, sensor properties, and calibration. Improving any of these factors will also decrease the absolute error. Accordingly, the approach yields an optimal result within the unavoidable tolerances. Assumption of maximum error in acceleration measurements would lead to pessimistic error bounds and conflict with the stochastic error model, where individual large errors are improbable, but possible.

A more useful approach to error analysis is to estimate the standard deviations for the speed and position. The measurement and observation errors ($\delta\boldsymbol{c}$) in measured data ($\boldsymbol{c}$) cause an error ($\delta\boldsymbol{x}$) to the estimated speed and position solved from the least squares problem. The error in measurement data and

the estimated speed and position are related by Eq. (7)

$$\delta \boldsymbol{x} = \left(\mathbf{D}^T\mathbf{D}\right)^{-1}\mathbf{D}^T\delta \boldsymbol{c}. \tag{7}$$

The covariances of linear combinations condition fulfill Eq. (8)[32;33]

$$V(\delta \boldsymbol{x}) = \left(\mathbf{D}^T\mathbf{D}\right)^{-1}\mathbf{D}^T V(\delta \boldsymbol{c})\mathbf{D}^T\left(\mathbf{D}^T\mathbf{D}\right)^{-1} \tag{8}$$

The covariance matrix $V(\delta \boldsymbol{c}) = \delta c\mathbf{I}$, where δc is the variance and $\mathbf{I}$ is identity matrix. Thus, Eq. (8) reduces to Eq. (9)

$$V(\delta \boldsymbol{x}) = \delta c\left(\mathbf{D}^T\mathbf{D}\right)^{-1} \tag{9}$$

The diagonal elements of $V(\delta \boldsymbol{x})$ are the variances of the error in estimated speed and position. In general, the square root of the variance is the standard deviation. In the test cases, δc was set to 10^{-4}. The standard deviations provide one with an estimate of the solution accuracy with respect to the measurement accuracy.

Video recordings All DP skiing tests were video recorded with two cameras (200 and 50 frames per second) placed on the side of the track. The cameras were synchronized and the skier's position was obtained in 200 frames per second accuracy with linear interpolation. The recording was used to calculate time intervals between designated marks on the track. The time stamps were determined manually from the video after the test, but technically, it would not be difficult to automate this (for example with open source imaging software libraries such as OpenCV[34], which runs also on mobile phones). For each run, the manual process took approximately 5-10 minutes, whereas an automated process (tested afterward in Adobe After Effects software) took only seconds to run.

Pole angle during poling phase (PP) was also determined from the video recordings. The horizontal component of the force is responsible for sustaining and accelerating forward motion, and ultimately

determining skiing speed. The vertical component of the pole force lifts the skier upward and has no direct effect on forward motion. The angles of both poles with respect to the vertical were determined in seven points during the push. Average evolution of pole angle was calculated separately for both grips as shown in Fig. 2. A fourth degree polynomial was fitted to the data (best fit in a least-square sense). As previously noted, this process can be automated with Adobe After Effects or OpenCV. An alternative to image processing is to embed angular velocity sensors to the grip to specify the pole angles.

The azimuthal angle of the camera induces parallax error to the pole angle. The magnitude of this error changes with respect to the skier's position during the push. Parallax error was compensated for with the information about camera position (distance from the track and height), azimuthal camera angle, elevation angle, and the skier's position in the video frame. Each pole was assumed to travel in a plane. Correction was made individually for each calculated pole angle. The greatest correction was 7.6 degrees.

The angle α between the pole and the vertical was used to divide the pole force F into vertical F_v and horizontal F_h components by using formulas $F_h = F\sin(\alpha)$ and $F_v = F\cos(\alpha)$.

Field testing

In order to determine whether the presented system can be used to measure differences in skiing speed and DP skiing characteristics caused by differences in equipment, the system was tested with two slightly different grip designs. The purpose was to demonstrate the measurement method and because only one participant was included in the study, a statistical comparison could not be done between the two grips. In addition, no claims about the superiority between the grips were made. A standard grip was tested against a custom made grip (Fig. 2). The custom grip has a mechanical hinge and a rigid lever instead of a flexible strap.

The participant was a top World Cup level cross-country skier (height 174 cm, weight 71 kg). The skier was familiar with both grips and informed of the procedures and potential risks associated with this study. The participant gave his written informed consent to participate. Research methods were approved by the university ethics committee.

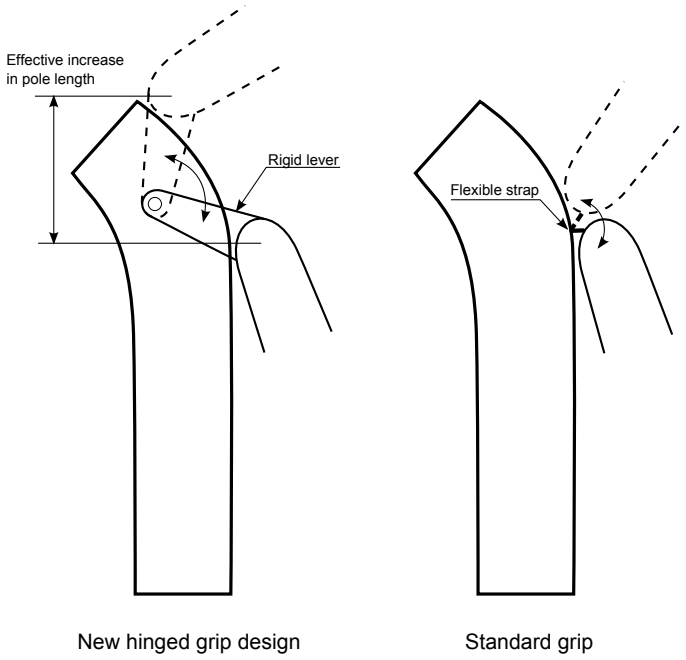

Figure 2. The new grip design compared to the standard grip.

The participant performed a DP skiing test session on an indoor running track with roller skis. The type of roller skis was ”slow”, designed for diagonal skiing, and accordingly, the bearings had a relatively high rolling resistance. The testing was conducted in the Pajulahti Sports Centre, Nastola. The tests were done at both submaximal (approximately 90% of maximum) and maximal velocity. In the submaximal velocity measurement, straight 100 m track was skied five times with both grips, first with the standard grip and then with the hinged grip. In the maximal velocity measurement, four repetitions were made with both grips.

The evaluated poling cycles were selected so that the skier had already accelerated. Furthermore, the skier attempted to maintain constant speed over all measured cycles. In total, the results were calculated for 20 poling cycles (in both submaximal and maximal velocity measurements) from several runs. The first cycle picked from each run was the one closest to the 40 m mark. Peak pole force (PPF), impulse of pole force (IPF), and horizontal impulse of pole force (IPF_h) were determined from the force data.

PPF is the maximum value of the force during the push, excluding the initial force peak caused by the pole-ground impact. IPF and IPF_h were calculated as an integral of the pole force and horizontal pole force (the angle between the pole and vertical was determined from video recordings) over PP duration, respectively. Values were calculated separately for both poles. The time characteristics measured for the poling cycle in this study were time of the poling cycle (CT), poling phase (PT), recovery phase (RT) and time to peak pole force ($TPPF$). Poling frequency (Pf) is the reciprocal of CT (i.e., $Pf = 1/CT$). A mean force curve of one push was determined for both grips.

The video cameras were positioned 50 m from the start point and at the 80 m mark. The camera at 50 m was panned during the runs, and the optical axes of the camera at the 80 m mark was aligned with the mark on the track. Distances 40 m and 60 m were marked to the track in the same manner, and the time stamps at these marks were obtained from the SMPTE [35] timecode of the video images. The average speed of the cycles was estimated from the inertial measurement data between starts of cycles for the same stretch as the force data (from approximately 40 m to 60 m). The only speed observation employed was the trivial zero initial speed, and hence, no additional speed observations took place.

The IMU and force sensors were synchronized before the test. The data logger of force sensors contained an accelerometer triad, which was synchronic with the force sensors. The data logger was placed on the top of the IMU and a knock was induced to the data logger. The knock creates a recognizable signal in the accelerometer data. The pole-ground impact was exploited to synchronize the force sensors and the two video recordings.

The load cell in the right pole broke during the maximum velocity measurement. The load cell in the left pole did not work properly with the standard grip and gave substantially lower values than the actual forces. Thus, the force measured for the left hand with standard grip and the right hand in maximal velocity measurement, were excluded. However, the cycle parameters and speeds could be calculated for all measurements.

All data is presented as means and standard deviations. All calculations and statistical analysis were made with MATLAB R2013a (MathWorks) and Excel 2010 (Microsoft).

Results

Average pole force curves for one PP (Fig. 3), force and cycle characteristics and skiing speed (Table 1) were determined. One poling cycle is divided into PP and recovery phase (RP). From the force point of view, PP starts with a significant force peak which is caused by the pole-ground contact. After the initial peak, force increases until reaching the maximum value (PPF). After that, the force decreases gradually until reaching zero at the end of PP. During RP, the skier lifts his centre of mass and prepares for the next PP.

Measurements showed difference in the shape of the force curves and in the measured force and cycle characteristics with the two grips. The results are presented in Table 1. The most significant differences were detected in PPF, Pf and RT. Force characteristics could not be compared in the maximal velocity measurement due to malfunctions in the measurement system.

No difference between grips was detected in the average speed (from approximately 40 m to 60 m) in either test. In the submaximal velocity test, average speeds were 23.0 ± 0.02 $\mathrm{km/h}$ and 23.0 ± 0.03 $\mathrm{km/h}$ and in the maximal velocity test, average speeds were 24.9 ± 0.03 $\mathrm{km/h}$ and 24.9 ± 0.02 $\mathrm{km/h}$ with standard and hinged grips, respectively.

The pole angle during one push in submaximal speed measurement is presented in Fig. 4(a). At the start of the push, the pole is in nearly a vertical position and the pole angle increases nearly linearly during the push. At the very end of the push, the angle stops increasing, or even slightly decreases, before the end of the ground contact.

The horizontal pole force in submaximal speed measurement is presented in Fig. 4(b). PP starts with the poles in nearly a vertical position, which greatly limits the horizontal force component in the early stages of the push. Horizontal force curves, as shown in Fig. 4(b), are different with different grips, although the difference was smaller than in the total force curves.

Instantaneous speed of the ski and the pole force for the submaximal and maximal velocity measurements are presented in Fig. 5(a, b). The maximum standard deviation in the instantaneous speed and position was ± 0.003 $\mathrm{m/s}$ and ± 0.022 m, respectively. There was considerable change in ski speed

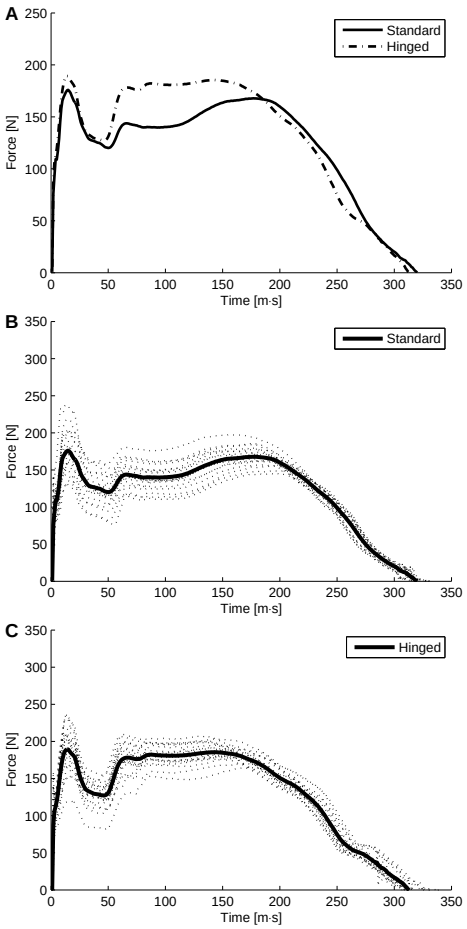

Figure 3. Average pole force curves for both grips in the submaximal velocity measurement (a) and individual force curves for both grips (b, c).

during the poling cycle. Average change in speed was 49.2% and 57.0% compared to the average speed in submaximal and maximal velocity tests, respectively. It should be noted that the speed of the ski differs considerably from the speed of the skier's centre of mass because the skier changes his position considerably during the PP.

Table 1. Pole force and cycle parameters for all measurements.

Measurement	Variables	Mean ± SD	
		Standard grip	Hinged grip
Submaximal velocity	Speed [km/h]	23.0±0.02	23.0±0.03
	CT [s]	0.93±0.03	0.94±0.03
	PT [s]	0.31±0.01	0.31±0.01
	RT [s]	0.61±0.03	0.63±0.02
	$TPPF$ [s]	0.19±0.01	0.15±0.01
	Pf [Hz]	1.08±0.04	1.06±0.03
	PPF [N]	168.9±12.6	187.6±9.2
	IPF [Ns]	39.0±3.5	41.8±2.6
	PPF_h [N]	158.3±10.4	163.9±6.2
	IPF_h [Ns]	30.0±2.4	30.2±1.8
Maximal velocity	Speed [km/h]	24.9±0.03	24.9±0.02
	CT [s]	0.68±0.03	0.67±0.03
	PT [s]	0.27±0.01	0.27±0.01
	RT [s]	0.41±0.03	0.40±0.02
	$TPPF$ [s]	0.17±0.01	0.13±0.01
	Pf [Hz]	1.47±0.07	1.49±0.04
	PPF [N]	–	165.1±11.4
	IPF [Ns]	–	32.2±2.6
	PPF_h [N]	–	137.0±7.6
	IPF_h [Ns]	–	21.6±1.8

CT [s], cycle time
PT [s], poling time
RT [s], recovery time
$TPPF$ [s], time to peak pole force
Pf [Hz], poling frequency
PPF [N], peak pole force
IPF [N s], impulse of pole force
PPF_h [N], horizontal pole force
IPF_h [Ns], horizontal impulse of pole force

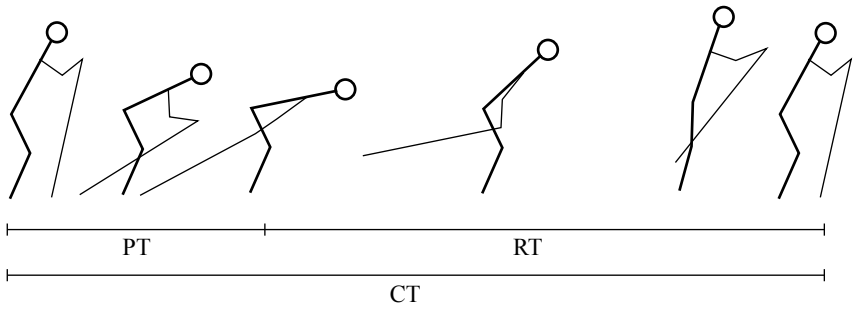

Discussion

The objective of the present study was to demonstrate the combination of simple field measurements to characterise skiing performance. The key quantities measured in this study were Pf, RT, impulses

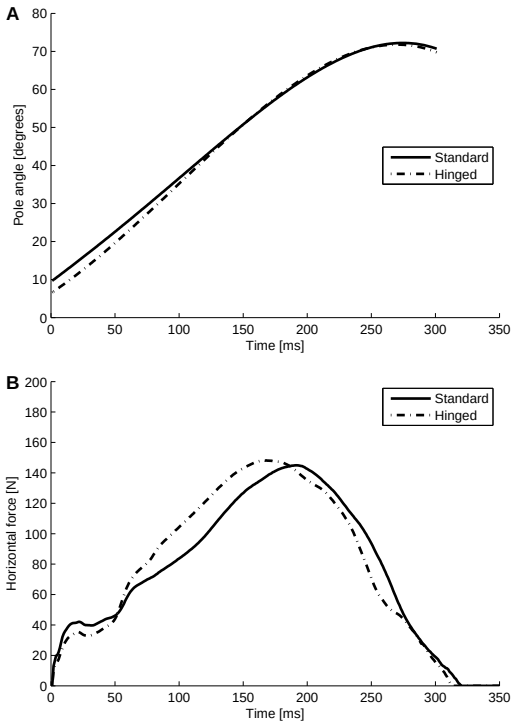

Figure 4. Average pole angle (a) and horizontal pole force (b) for both grips in the submaximal speed test.

(IPF and IPF_h) and skiing speed. These are subsequently used to estimate skiing economy, maximum performance, and differences in ski equipment. As a method, pole force measurements and augmented inertial speed measurements recordings appeared to be appropriate for determining these characteristics in field conditions with DP technique. Both pole force and inertial measurement systems are portable and can easily be used in any location. In this case, video recordings were used to augment the inertial measurement, but also other methods, such as global navigation satellite system (GNSS)[36;37] or light gates, could be used.

In the field test, no difference in the average speed was detected between the grips in either test. In the case of the submaximal speed test, this means that the athlete could maintain constant effort during

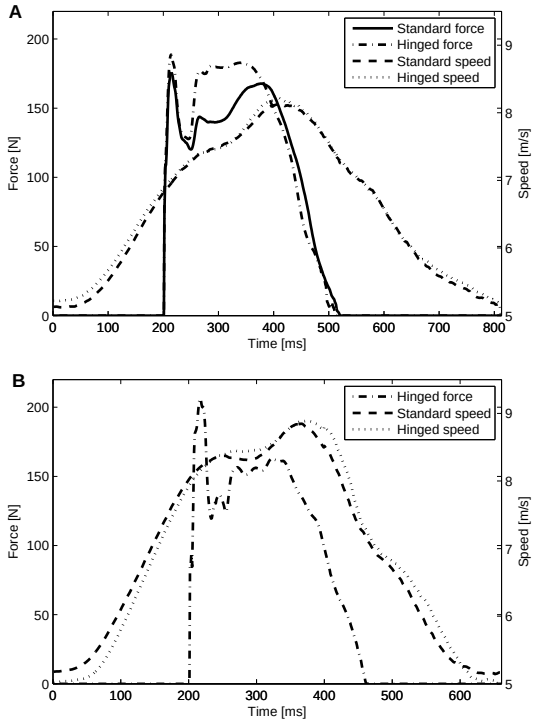

Figure 5. Pole force and ski speed in submaximal velocity (a) and maximal velocity (b) measurements.

the test and the differences in force and cycle characteristics could be used for estimating difference in economy. In the maximum speed test, there was no difference in maximum performance between the grips, since the speed was the same for both grips.

In DP, a technique characterized by low poling frequency, long cycle length and high impulse with each push is related to better work economy and thus better performance in long distances.[9;11] The skier does a substantial amount of internal work at each poling cycle due to repositioning.[38 as cited in 9] This internal work is reported to represent approximately 30% of the total energy consumption.[38 as cited in 9] For that reason, lower Pf and longer RT are related to longer time to exhaustion due to a lower heart rate response and blood lactate concentration.[8]

In the example case, there seemed to be noticeable difference in the temporal forces during the polling cycle. Lower Pf and longer RT were detected with the hinged grip in constant speed tests. Higher impulse was also detected, which is in line with the observed cycle characteristics. No speed difference was detected between the grips. Thus, the method seems suitable for detecting differences between different ski equipment, suggesting there are differences between the two grips. However, further research with more participants and in different conditions is needed to validate these results.

A slight difference was also detected in the shape of the instantaneous speed curves. This difference in ski speed implies a difference in the push with different grips. However, the instantaneous speed of the centre of the mass cannot be directly obtained with this method, as it is impossible to attach the IMU to the centre of mass of the skier, because its position changes constantly. For this reason, the translational power for the centre of the mass of the skier could not be estimated, which is unfortunate, since it would give information about the performance of the skier in field conditions.

Although the inertial system enables more precise speed measurements, it adds an extra layer on the measurement procedure. Measurements have to be augmented with additional observations about the skier's position and/or velocity along the track. Thus, some supporting measurements are needed. With additional observations, speed can be solved as a boundary value problem. Solving the speed as an initial value problem would give poor results, since the errors in measured acceleration accumulate to the position and speed estimates with time.[39] Analysing the data and calculating results also requires more work than would be required with a light gate system.

In this study, the inertial measurement was used for measuring skiing speed in order to estimate performance and difference between two different grip designs, but it also has other potential uses in cross-country skiing studies. Information about the ski speed could be used, for instance, to compare the glide properties of different skis in DP. If a skier has the same horizontal (impulse of) pole force with different skis, but the skiing speed is greater with a given pair of skis, then this pair has better glide properties in DP. If the same skiing speed is achieved with a smaller horizontal force with a given pair

of skis, then this pair can be considered better. This cannot be demonstrated in this study, since the same roller skis were used in the tests.

Conclusion

In this study, fusion of pole force measurements, inertial measurements, and video recordings were exploited to compare cross-country skiing performance and find differences in ski equipment in field conditions. Special interest was focused on the use of inertial measurements with additional position observations to estimate instantaneous and average speed in cyclic motions of DP. As a result, this study demonstrated that the presented system can be used to find differences in speed and cycle parameters of DP skiing characteristics, as well as two different grip designs, which were exploited in the tests. In addition, the cycle parameters and speed were further exploited to determine whether there were differences in the maximum performance. Also, the concept to compare glide properties of the skis in DP was introduced. After this initial proof of concept, further development should focus on using alternative methods (i.e., GNSS) for inertial measurement augmentation. Exclusion of the video camera would make the system simpler and feasible to use on longer distances along an arbitrary track. These initial tests lay the foundation for future development of light and portable performance measurement systems for coaches and equipment manufacturers.

Acknowledgements

The authors thank the athlete for his participation, enthusiasm and cooperation and the Pajulahti Sports Center for providing facilities for indoors testing.

Declaration of conflicting interests

The authors declare that there is no conflict of interests.

Funding

Our institution got monetary support for this submitted work from the Finnish national technology agency TEKES, which is a governmental organization. For the tests, we received material support, including poles and roller skis, from One Way Sport Oy, Finland.

References

1. Minetti AE. Passive tools for enhancing muscle-driven motion and locomotion. *J Exp Biol* 2004; 207: 1265–1272.
2. Vähäsöyrinki P, Komi PV, Seppälä S, et al. Effect of skiing speed on ski and pole forces in cross-country skiing. *Med Sci Sports Exerc* 2008; 40: 1111–1116
3. Nilsson J, Jakobsen V, Tveit P, et al. Pole length and ground reaction forces during maximal double poling in skiing. *Sport Biomech* 2003; 2: 227–236.
4. Stöggl T, Holmberg H–C. Force interaction and 3D pole movement in double poling. *Scand J Med Sci Sport* 2011; 21: 393–404.
5. Nilsson J, Tinmark F, Halvorsen K, et al. Kinematic, kinetic and electromyographic adaptation to speed and resistance in double poling cross country skiing. *Eur J Appl Physiol* 2013; 113: 1385–1394.
6. Göpfert C, Pohjola M, Linnamo V, et al. Forward acceleration of the centre of mass during ski skating calculated from force and motion capture data. *Sports Eng* 2017; 20: 141–153.
7. Holmberg H–C, Lindinger S, Stöggl T, et al. Biomechanical analysis of double poling in elite cross-country skiers. *Med Sci Sport Exerc* 2005; 37: 807–818.
8. Holmberg H-C, Lindinger S, Stöggl T, et al. Contribution of the legs to double-poling performance in elite cross-country skiers. *Med Sci Sport Exerc* 2006; 38: 1853–1860.
9. Lindinger S, Stöggl T, Müller E, et al. Control of speed during the double poling technique performed by elite cross-country skiers. *Med Sci Sport Exerc* 2009; 41: 210–220.
10. Lindinger S, Holmberg H–C, Müller E, et al. Changes in upper body muscle activity with increasing double poling velocities in elite cross-country skiing. *Eur J Appl Physiol* 2009; 106: 353–363.

11. Stöggl T, Lindinger S, Müller E. Analysis of a simulated sprint competition in classical cross country skiing. *Scand J Med Sci Sport* 2007; 17: 362–372.
12. Heil DP, Engen J, Higginson BK. Influence of ski pole grip on peak upper body power output in cross-country skiers. *Eur J Appl Physiol* 2004; 91: 481–7.
13. Bojsen-Møller J, Losnegard T, Kemppainen J, et al. Muscle use during double poling evaluated by positron emission tomography. *J Appl Physiol* 2010; 109: 1895–1903.
14. Fasel B, Favre J, Chardonnens J, et al. An inertial sensor-based system for spatio-temporal analysis in classic cross-country skiing diagonal technique. *J Biomech* 2015; 48: 3199–3205.
15. Breitschädel F, Berre V, Andersen R, et al. A comparison between timed and IMU captured Nordic ski glide tests. In: *9th Conference of the International Sports Engineering Association (ISEA)* 2012; 34: 397–402.
16. Myklebust H, Losnegard T, Hallén J. Differences in V1 and V2 ski skating techniques described by accelerometers. *Scand J Med Sci Sport* 2014; 24: 882–893.
17. Losnegard T, Myklebust H, Skattebo Ø, et al. The Influence of Pole Length on Performance, O_2-Cost and Kinematics in Double Poling. *Int J Sports Physiol Perform* 2017; 12: 211-217
18. Myklebust H, Øyvind G, Jostein H. Validity of ski skating center-of-mass displacement measured by a single inertial measurement unit. *J Appl Biomech* 2015; 31: 492–498.
19. Losnegard T, Myklebust H, Ehrhardt A, et al. Kinematical analysis of the V2 ski skating technique: A longitudinal study. *J Sports Sci* 2017; 35: 1219–1227
20. Mahood N V., Kenefick RW, Kertzer R, et al. Physiological determinants of cross-country skiing performance. *Med Sci Sport Exerc* 2001; 33: 1379–1384.
21. Bortolan L, Pellegrini B, Frederico S. Development and validation of a system for poling force measurement in cross-country skiing and nordic walking. In: *ISBS-Conference Proceedings Archive 2009* (eds Harrison AJ, Anderson R, Kenny I), Limerick, Ireland, 2009.
22. Strain measurement devices. S400-button load cell. Online Referencing, http://www.smdsensors.com/Products/S400-Button-Load-Cell/ (2017, accessed 19 Jan 2017).

23. Särkkä O, Nieminen T, Suuriniemi S, et al. Augmented inertial measurements for analysis of javelin throwing mechanics. *Sports Eng* 2016; 19: 219–227.
24. Titterton D, Weston JL. *Strapdown inertial navigation technology.* American Institute of Aeronautics and Astronautics, 2004, pp. 17–57.
25. Analog Devices. ADXL326 Accelerometer. Online Referencing, `http://www.analog.com/static/imported-files/data_sheets/ADXL326.pdf` (2017, accessed 19 Jan 2017)
26. STMicroelectronics. LPY4150AL MEMS motion sensor. Online Referencing, `https://media.digikey.com/pdf/Data Sheets/ST Microelectronics PDFS/LPY4150AL.pdf` (2017, accessed 19 Jan 2017).
27. Särkkä O, Nieminen T, Suuriniemi S, et al. A multi-position calibration method for consumer-grade accelerometers, gyroscopes, and magnetometers to field conditions. *IEEE S Journal* 2017; 17: 3470–3481
28. Chatfield AB. *Fundamentals of high accuracy inertial navigation.* American Institute of Aeronautics and Astronautics, 1997.
29. Nieminen T. *A non recursive solution method for fixed interval smoothing problem applied to short-term inertial navigation.* PhD Thesis, Tampere University of Technology, Tampere, 2013. pp. 1–68.
30. Iserles A. *A first course in the numerical analysis of differential equations.* Cambridge University Press, 1996.
31. Hayashi F. *Econometrics.* Princeton University Press, 2000.
32. Lindgren BW. *Statistical Theory*, 3rd ed. New York: MacMillan, 1976.
33. Aster RC, Borchers B, Thurber CH. *Parameter estimation and inverse problems*, 2nd ed. Academic Press, 2013.
34. http://opencv.org
35. https://en.wikipedia.org/wiki/SMPTE_timecode
36. Farrell JA, Barth M. *The global positioning system & inertial navigation.* McGraw-Hill, 1999.
37. Grewal MS, Weill LR, Andrews AP. *Global positioning system, inertial navigation, and integration.* John Wiley & Sons, 2001.
38. Holmberg H–C. *The physiology of cross-country skiing: With special emphasis on the role of the upper body.* PhD Thesis, Karolinska Institutet, Stockholm, 2005.

39. Nieminen T, Kangas J, Suuriniemi S, et al. Accuracy improvement by boundary conditions for inertial navigation, *Int J Nav Obs* 2010.

A list of figure captions

Figure 1. The force measurement device (a), the IMU (b), and the calibration equipments (c).

Figure 1 (a). A separate load cell can been seen below the poles. The data logger is above right. Above left is the standard grip and below left is the hinged grip, which both were used in the field tests.

Figure 1 (b). The roller ski with the IMU in front of the binding.

Figure 1 (c). The calibration stand (on the left) and the cube (on the right) were exploited to calibrate the load cells and inertial sensors, respectively.

Figure 2. The new grip design compared to the standard grip.

Figure 3. Average pole force curves for both grips in the submaximal velocity measurement (a) and individual force curves for both grips (b, c).

Figure 4. Average pole angle (a) and horizontal pole force (b) for both grips in the submaximal speed test.

Figure 5. Pole force and ski speed in submaximal velocity (a) and maximal velocity (b) measurements.

A list of notation

a	Acceleration
b	Bias
$\boldsymbol{b}$	Vector, which entries are acceleration measurements
c	Scale factor
$\boldsymbol{c}$	Vector, which is compilation of $\boldsymbol{b}$, $\boldsymbol{v}^\star$, and $\boldsymbol{p}^\star$
h	Time step between successive measurements
p	Position
$\boldsymbol{p}^\star$, $\boldsymbol{v}^\star$	Vectors, which entries are additional position and speed observation
$\boldsymbol{r}$, $\boldsymbol{r}_1$, $\boldsymbol{r}_2$	Residual vectors
v	Speed
x	Pole force due to standard weight
$\boldsymbol{x}$	Vector, which entries are position and speed
y	Measured pole force
α	Angle between pole and the vertical
δc	Variance of the measurement errors
$\delta\boldsymbol{c}$	Vector, which entries are measurement and observation errors
$\delta\boldsymbol{x}$	Vector, which entries are errors in estimated speed and position
$\mathbf{A}$	Matrix, which depends on h
$\mathbf{B}$, $\mathbf{C}$	Binary matrixes
$\mathbf{D}$	Matrix, which is compilation of $\mathbf{A}$, $\mathbf{B}$, and $\mathbf{C}$
F	Pole force (calibrated)
F_h	Horizontal pole force
F_v	Vertical pole force
$\mathbf{I}$	Identity matrix
N	Number of time instances